

Validation of a simplified computer simulation method for plastic forming of metals by conventional tensile tests

<http://dx.doi.org/10.1590/0370-44672015700039>

Daniel Fraga Pinto

Professor de Ensino Básico, Técnico e Tecnológico
Instituto Federal de Minas Gerais - IFMG
Campus Ouro Preto - Coordenadoria de Metalurgia
Ouro Preto - Minas Gerais - Brasil
danielfp10@yahoo.com.br

Maria Aparecida Pinto

Professora Associada
Universidade Federal de Ouro Preto - UFOP
Escola de Minas
Departamento de Engenharia Metalúrgica e de Materiais
Ouro Preto - Minas Gerais - Brasil
mariap@em.ufop.br

Paulo Raimundo Pinto

Professor de Ensino Básico, Técnico e Tecnológico
Instituto Federal de Minas Gerais - IFMG
Campus Ouro Preto - Coordenadoria
de Controle e Automação
Ouro Preto - Minas Gerais - Brasil
paulo.pinto@ifmg.edu.br

Adilson Rodrigues da Costa

Professor Associado
Universidade Federal de Ouro Preto - UFOP
Escola de Minas
Departamento de Engenharia Metalúrgica e de Materiais
Ouro Preto - Minas Gerais - Brasil
adilson@em.ufop.br

Abstract

This work was developed in order to validate a simplified computer simulation method for application in the drawing processes. The results of tensile tests on AISI 1004, AISI 1020 steel and copper were compared to those of computer simulations performed using the Deform-3DTM software. Each specimen was assumed to be an elasto-plastic material and was meshed with 50,000 finite elements. Young's modulus and Poisson's ratio were the only material properties considered in the elastic region; the parameters of Hollomon's equation were used in the plastic region up to constriction. A strain rate of $1 \times 10^{-3} \text{ s}^{-1}$ was applied during the simulations. In the plastic region, up to the point of constriction, the curves obtained from the simulations showed reasonable correspondence to those determined from physical testing. However, the former diverged from the latter in the elastic and elastic-plastic transition regions. This divergence indicates that microstructural factors may have a greater influence in the transition region than in the plastic region. Moreover, the correlation obtained in the plastic region indicates that the proposed method has the potential to be applied in drawing processes.

Keywords: tensile test; computer simulation; finite element method.

1. Introduction

The use of computer simulation based on the finite element method (FEM) to investigate the strain mechanisms in plastic forming processes has been a source of interest for many researchers (MARANGONI and MASSAROPPI JR. (2016); HUAN & LU, 2010; HE *et al.*, 2003; MATH, 2002). This interest stems mainly from an increase in the predictive capacity of numerical methods and computer-aided engineering tools. Such increased capacity allows computer simulation-based project checks that are cheaper and simpler than those associated with physical tests on prototypes (KADKHODAYAN & MOAYYEDIAN,

2011).

The simulation-determined solutions must, however, be compared to those of the physical tests in order to apply the method with sufficient precision to the analysis of plastic forming processes such as lamination, drawing, stamping, forging, etc.

FEM-based computer simulation programs have been used to analyze the behavior of materials during forging and deep stamping. Studies by Marangoni and Massaroppi Jr. (2016), Santos and Martins (2016) and Huan & Lu (2010) are particularly noteworthy because their results significantly improved the under-

standing of the process, especially with regards to the strain analysis performed by employing the FEM.

Although the use of numerical methods in engineering has benefitted greatly from advances in both computer software and hardware, physical tests must be used to ultimately confirm the applicability of the calculated solutions. Huang & Lu (2010) highlighted the importance of verifying, in practice, the proximity of numerical results to the experimental data of the forming process under study. This check indicates whether the formulation used is suitable for the study in question or if modifications are required.

The aim of this work, therefore, is to validate a simple, fast, and reliable computer simulation method for use in metal plastic forming processes, particularly drawing, by using the Deform3DTM simulation program.

Materials are most simply strained using a pure tensile stress method. In this process, specimens are strained without externally imposed restrictions, and the bars undergo uniform strain until constriction begins. Furthermore, the simplest method to determine the stresses involved in drawing assumes that the drawing tension is obtained by means of a one-dimensional tensile stress. The tension required for drawing the material must, however, be lower than the yield strength of the bar that has passed through the die (CETLIN & HELLMANN, 2005).

To this end, the tensile test now constitutes an important tool for valida-

tion of the simulation methods proposed for studies of the drawing process. In addition, the strain mechanisms involved in the conventional uniaxial tensile test are already well understood and, as such, this test constitutes a suitable reference for validating the proposed simulation methodology.

It is important to note that the present study is an integral part of a larger project that will enable the investigation of the stresses involved and the strain mechanisms governing the drawing process of metals and metallic alloys. More importantly, the information obtained via computer simulation using the Deform3DTM program may constitute yet another tool for optimizing the drawing process of steel, thereby reducing the cost and time of analysis.

Therefore, a conventional uniaxial tensile test is simulated using the FEM-

based Deform3DTM calculation code in order to obtain the stress-strain curves of the materials considered. The yield strength, ultimate tensile strength, and percent elongation, determined from the curves obtained in the simulations, are compared to the values from the physical tensile tests. Moreover, analysis of the results indicate whether the formulation used is suitable for the study in question or if adjustments are needed.

Although significant deviations have resulted for some metals (SANTOS, 2005), Holloman's empirical equation (equation 1) is typically used to describe the behavior of materials in the plastic region up to the point of constriction. This work validates the hypothesis that the behavior of the material in the elastic and plastic regions are governed by Hooke's law and Holloman's equation (equation 1), respectively.

$$\sigma_v = K \times \epsilon^n \tag{1}$$

In equation 1, σ_v is the true stress, ϵ is the true strain, k is the strength coefficient that quantifies the level of strength of the material, and n term is the hardening exponent, which represents the ability of the material to distribute the strain (CETLIN & HELLMANN, 2005).

2. Materials and methodology

Uniaxial tensile tests were performed on machine wire specimens of AISI 1004 steel, AISI 1020 steel, and commercial copper wire C110, with a circular cross-section of 6.5 mm in diameter, in order to determine their respective stress-strain curves. The values of the yield strength, ultimate tensile strength, and percent elongation were determined from the curves and compared to those obtained from computer simulations. In addition, the chemical composition and microstructure of the samples of each material

were determined by optical emission spectrometry and examined using optical microscopy, respectively.

Tensile tests were conducted in accordance with the ASTM E8M-04 standard. Five tensile tests were conducted on each of the materials, and the mechanical property values presented represent the arithmetic mean of the five tests.

The computer simulation step was performed using the Deform3DTM calculation code, which is based on the finite element method; Deform3DTM was developed mainly for the analysis

of metal plastic forming operations.

In the simulations, the specimens were assumed to be defect-free, elasto-plastic, and homogeneous materials, i.e., microstructural parameters were not taken into consideration.

Furthermore, Young's modulus and Poisson's ratio, obtained from literature and listed in Table 1, were the only material properties used in the elastic region. For the plastic yield, Holloman's equation (equation 1) was thought to adequately represent the phenomena involved.

	AISI 1004	AISI 1020	Copper
Young's Modulus (MPa)	210,000	210,000	120,000
Poisson's ratio	0.30	0.30	0.34

Source: Garcia (2012)

Table 1
Parameters used in computer simulations for the conventional tensile test.

In the plastic region, it was assumed that the relationship between the stress and the strain follows equation 1, up to the point of constriction. The k and n values for each material were obtained from the conventional tensile tests, in accordance with the ASTM E646-07 standard.

Araújo (2009) proposed a different, simpler, and faster method of obtaining

the k and n parameters compared to that proposed by the standard. According to the proposed method, the k and n parameters can be determined from the stress-strain curve by means of linear regression in the range of 10% of the plastic strain to constriction. The regression was performed using a $y = ax^b$ type power function, similar to Hollomon's equation (equation

1). This methodology was also used in the present study for comparison with the procedure proposed by the ASTM E646-07 standard.

The simulations were run in 1,000 steps, with automatic re-meshing after every 10 steps and integration time of 0.1s. Error thresholds of 0.05 and 0.005 were set for the strength and velocity, re-

spectively. Moreover, the frequently used Newton-Raphson mode of iteration was adopted since it usually converges in fewer iterations than other available methods (MENEZES, 2015; SANTOS, 2005).

The mesh was constructed from 50,000 tetrahedral finite elements based on a study of the influence of the number of ele-

ments in the mesh on the simulation of the drawing process (LAUDARES *et al.*, 2004). The mesh was generated using the default mesh-generation procedure in the program.

In addition, the stress was applied by the upper claw in order to achieve a constant strain rate of $1 \times 10^{-3} \text{ s}^{-1}$; the claw was programmed to move at the same

velocity as that used in the physical tests.

A rupture criterion (Equation 2) was selected from among the criteria proposed by the simulation program. According to this criterion, the specimen breaks when the integral of the $\sigma(\epsilon)$ function, which represents the flow curve of the material, reaches a critical value.

$$\int_{\epsilon_f} \sigma d\epsilon = \text{critical value} \quad (2)$$

As such, the $\sigma(\epsilon)$ function of each material was determined by substituting into equation 1, the k and n parameters that were obtained in the tensile tests. The calculation result of this integral

was then used as the rupture criterion for the simulations.

Furthermore, the stress-strain curves for each material were obtained based on the applied load (N) and dis-

placement (mm) values from the simulations. The simulations were performed in the laboratory of computational simulation of the DEMET/REDEMAT/EM/UFOP.

3. Analysis and discussion of the results

The chemical compositions of the materials used in this study are listed in Table 2.

Table 2
Chemical composition
of the analyzed materials (% by weight).

Materials	%C	%Mn	%S	%P	%Si
AISI 1004	0.037	0.227	<0.0050	0.0188	0.012
AISI 1020	0.177	0.817	0.0236	0.0180	0.160
	%Cu	%Ag	%Mn	%Ni	%Cr
ETP Copper	99.98	0.0061	0.0001	0.0031	0.00027

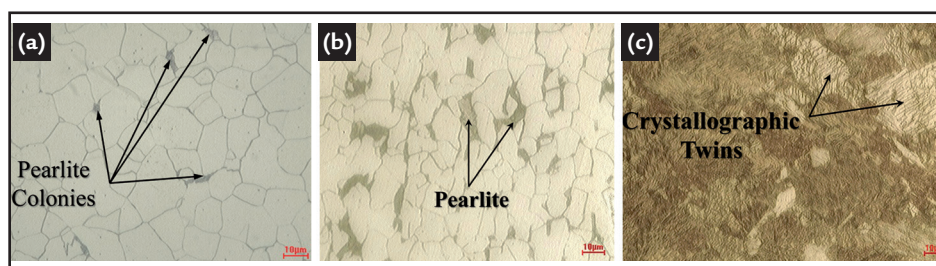
Microstructural parameters are neglected in the simulations. However, microstructural characterization of the material is necessary since the occurrence of highly heterogeneous microstructures can invalidate the hypothesis of uniform microstructures. Figure 1 shows the microstructures

observed in the longitudinal section of the analyzed materials. The AISI 1004 steel (Figure 1(a)) has a uniform grain structure, a few pearlite colonies and dispersed inclusions.

Compared to its AISI 1040 counterpart, the AISI 1020 steel (Figure 1(b)) also has a uniform grain structure and

dispersed inclusions but with an expectedly higher, albeit slightly, amount of pearlite owing to its higher carbon content (Table 2). In addition, the copper (Figure 1(c)) sample consists of finer grains than those observed in the steel specimens and crystallographic twin bands which are aligned in a particular direction.

Figure 1
Microstructures of the (a) AISI 1004 steel, (b) AISI 1020 steel, and (c) copper.



The result of the physical uniaxial tensile tests is presented in Figure 2.

Figure 2
Physical tensile test
results showing the stress-strain
curves for the materials analyzed.

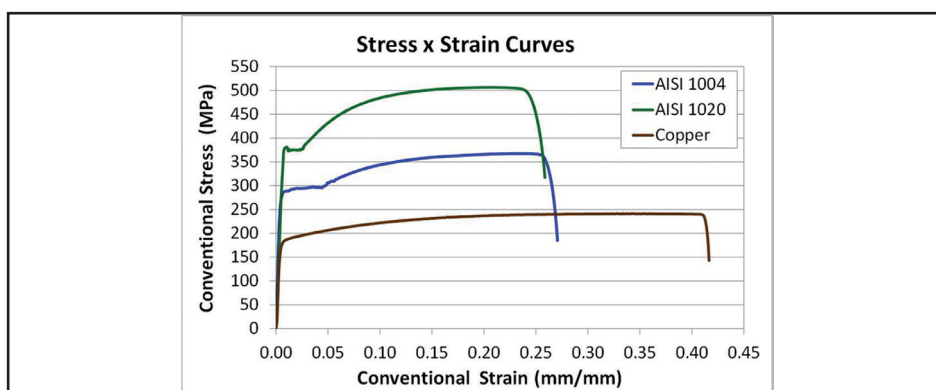


Figure 2 shows that the AISI 1004 steel has a more well-defined yield point than that of its AISI 1020 counterpart, which has a higher amount of carbon.

Furthermore, the true stress-true strain curve, the hardening exponent n , and the strength coefficient k were determined according to both the ASTM E646-07 standard and the pro-

cedure introduced by Araújo. Figure 3 compares the results obtained from both methods; the data points of each material are overlain by their respective trend lines.

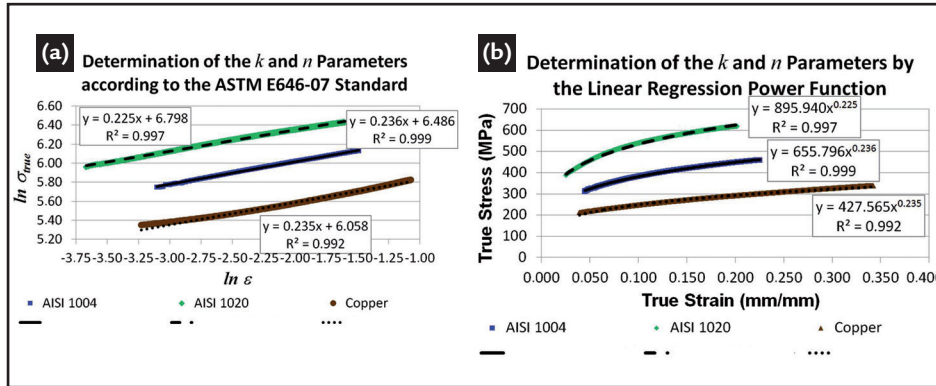


Figure 3 Determination of the k and n parameters from conventional physical tensile tests as stipulated by the (a) ASTM E646-07 standard and (b) linear regression proposed by Araújo (2009). σ_{true} : true stress; ϵ : true strain.

The trend lines in Figure 3(a) are linear, i.e., of the type $y=ax + b$, where the coefficient (slope of the line) a and the intercept b represent the hardening exponent n

and the strength coefficient k , respectively. Conversely, the trend lines in Figure 3(b) are defined by $y = ax^n$, and are, therefore, similar to Hollomon's equation (equation 1), which

describes the behavior of the material in the plastic regime up to the point of constriction. The k and n values were extracted from Figure 3 and subsequently compared (Figure 4).

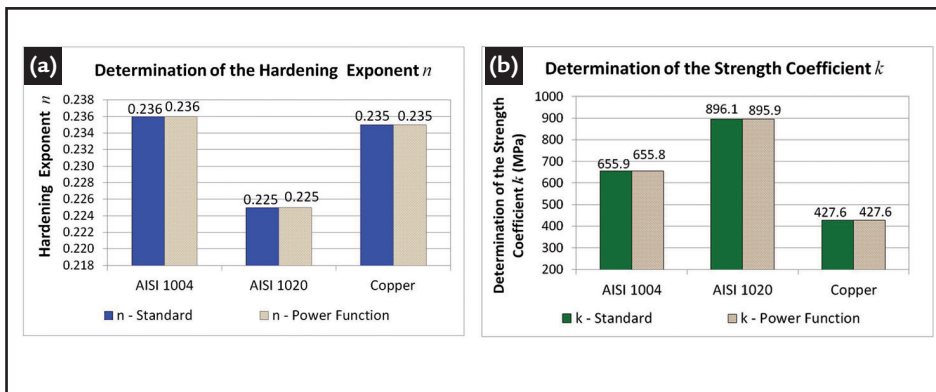


Figure 4 Comparison of the (a) n and (b) k parameters obtained from conventional physical tensile tests by using the ASTM E646-07 standard and the linear regression, power function proposed by Araújo (2009).

Figure 4 shows that, for all three materials, the values of k and n obtained in accordance with the ASTM E646-07 standard are similar to those determined by linear regression using the power-type function. These results

also confirm that, like the former, the simpler and more quickly applied methodology of the latter can be used to determine the values of k and n .

The properties of the three materials and their respective flow curves

were determined from the results of the physical uniaxial tensile tests (Figures 2 and 3) and are listed in Table 3. These flow curves were used as inputs to the calculation code of the simulation program.

Table 3 Mechanical properties and the respective flow curves obtained from the physical uniaxial test.

	σ_{ys} (MPa)	σ_{uts} (MPa)	% Elong.	Flow Curve
AISI 1004	294	372	27.0	$\sigma = 656 \times \epsilon^{0.236}$
AISI 1020	380	505	26.0	$\sigma = 896 \times \epsilon^{0.225}$
Copper	188	241	41.5	$\sigma = 428 \times \epsilon^{0.235}$

σ_{ys} : yield strength (0.2%);
 σ_{uts} : ultimate tensile strength;

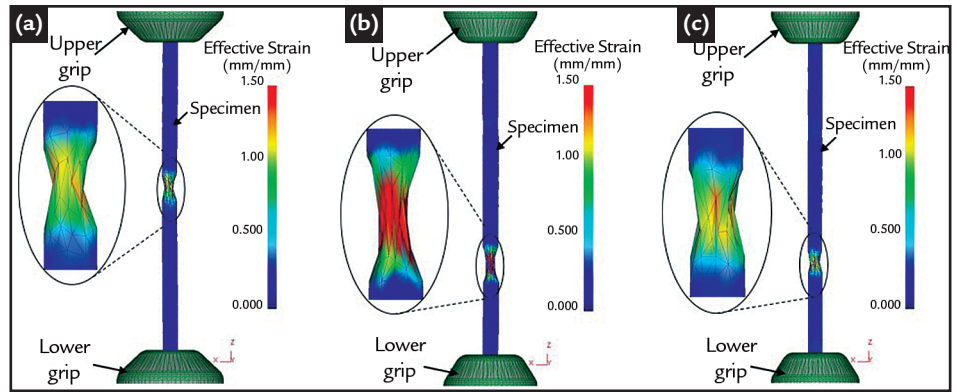
Elong.: percent elongation;

Figure 5 compares the simulation results for specimens on the verge of rupture. The figure also shows details of the region of rupture and the behavior of

the finite elements. As the figure shows, each specimen breaks after constriction in accordance with the rupture criterion adopted. However, rupture did not

always occur in the central region of the specimens, despite these materials having been considered homogeneous and defect-free.

Figure 5
Results of the computer simulations for specimens on the verge of rupture, detailing the rupture region in (a) AISI 1004, (b) AISI 1020, (c) Electrolytic-tough-pitch (ETP) copper.

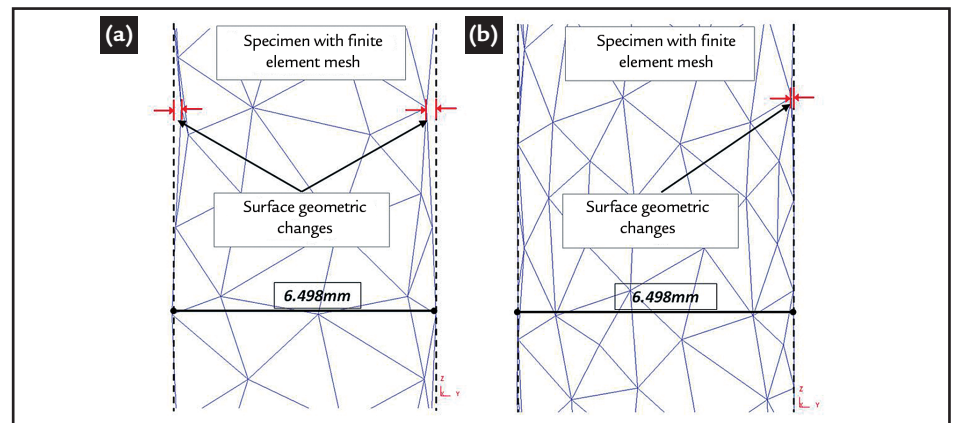


This inconsistency, as it relates to the location of the rupture, results possibly from the tetrahedral geometry of the finite elements that compose the mesh. The tetrahedral geometry of the elements makes it difficult to obtain a cylindrical sample

surface (represented by the dashed line in Figure 6). The simulated specimens have, instead, a corrugated surface that consists of discontinuous regions resulting from deviations of the element mesh from the cylindrical surface.

Although an increase in the number of finite elements in the mesh tends to resolve this issue, such superficial changes to the specimens lead to incorrectly defined boundary conditions, which, in turn, reduce the accuracy of the method.

Figure 6
Representation of the tetrahedral element mesh generated in the specimen and alteration of the solid surface in relation to the cylindrical surface of the sample in a mesh consisting of (a) 25,000 and (b) 50,000 finite elements.



Laudares *et al.* (2004) examined the influence of the number of finite elements in the mesh on the simulation of the drawing process for steel. The current work was conducted with 50,000 finite elements, which is ten times greater than that suggested by Laudares *et al.* (2004) as being a suitable representation of the material. Despite using 50,000

elements, regions that do not accurately represent the desired geometry could still be observed.

In addition to reducing the accuracy of the method, changes in the geometry promoted the concentration of tensions in certain regions of the specimen. As a result, these regions became preferred sites for the nucleation and

development of cracks and the ensuing rupture of the specimens. Rupturing in the non-central regions of the specimens may be attributed to this concentration of tensions.

Figure 7 shows the comparison between the stress-strain curves obtained from the physical tensile tests and the computer simulations.

Figure 7
Comparison between the stress-strain curves obtained from the physical tests and the computer simulations of the tensile test for (a) AISI 1004 steel, (b) AISI 1020 steel, and (c) copper.

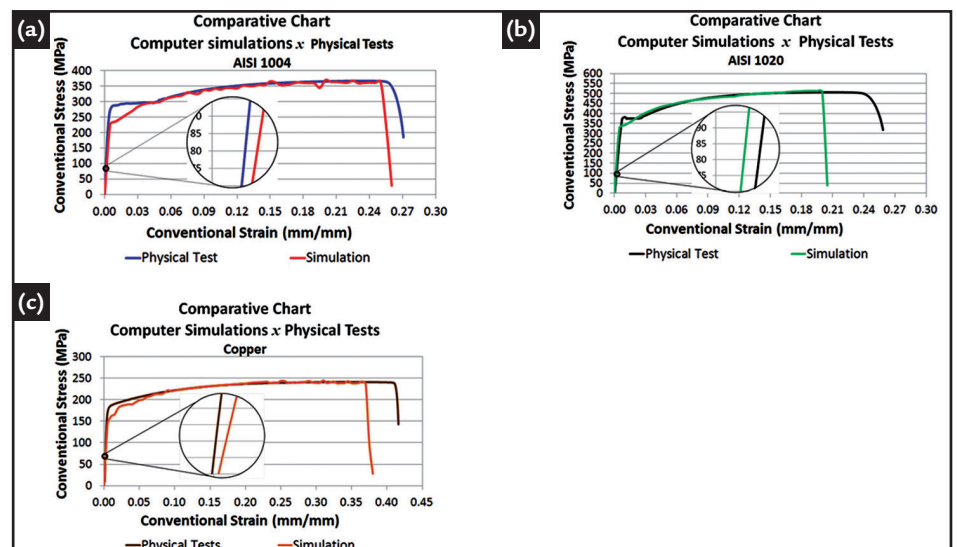


Figure 7(a), (b), and (c) reveal a reasonable correspondence between the curves in the region of 10% of the plastic strain to constriction, where Hollomon's equation (Equation 1) is valid.

However, there was small divergence between the curves in the elastic region. In fact, an enlarged view of the elastic region reveals a divergence of the curves.

The same behavior can be observed in the transition region between the elastic and plastic regimes, especially in the materials which have well-defined yield points.

Thus, if the analyses of the process under study are restricted only to the plastic region, that is, if the information from the elastic and the early yield regions are neglected, then this method can be applied

precisely and quickly.

The values of the yield strength (0.2%), ultimate tensile strength, and percent elongation of each material were also determined from the computer simulations. The values obtained from the simulations were compared with those from the physical tensile tests and the respective percentage errors are shown in Figure 8.

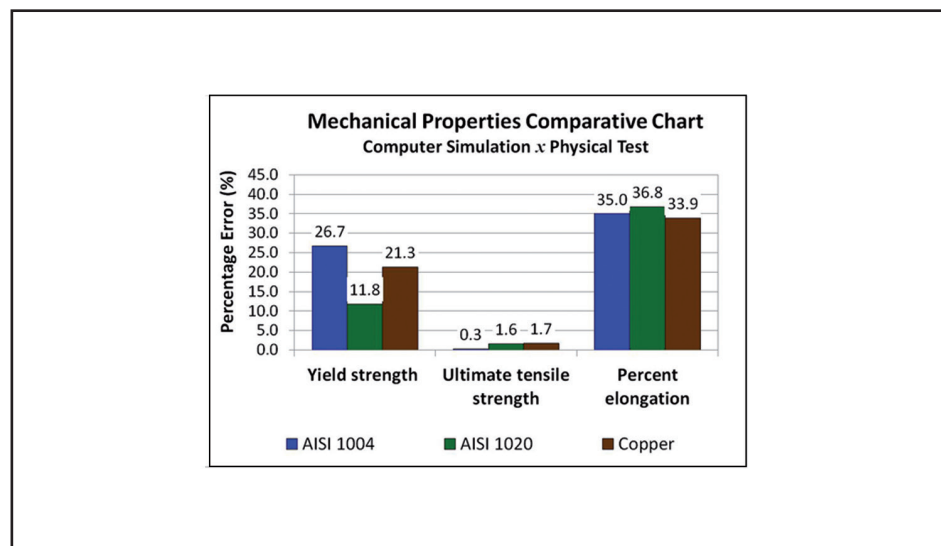


Figure 8
Percentage error of the mechanical properties obtained from the physical and computer-simulated tensile tests.

Figure 8 reveals a significant difference between the values obtained from the simulations and their physical test counterparts. In fact, the percentage error of the yield strength (0.2%) and the percent elongation exceed 11% and 35%, respectively for all three materials. These large differences in the yield strength values were expected since there was no correspondence between the tensile curves in the elastic region and in the transition region from the elastic to the plastic regime.

However, the percentage error of the

tensile strengths was less than 2%, which indicates a very reasonable correspondence between the values determined from physical measurements and those obtained from computer simulations.

In contrast, the elongation values obtained from the simulations are about 35% lower than those of the physical tests (Figure 8).

This difference stemmed from the fact that the material elongation in the simulations is strongly influenced by the rupture criterion adopted (equation

2). For each material analyzed, this criterion was defined by equation 1, using the k and n parameters obtained in the physical tensile tests. Hence, the rupture criterion adopted only the integration of the function relating to the plastic region of the curve, and neglected the contribution relating to the elastic region. This difference in the contributions considered, resulted in an influence on the elongation behavior of the materials, which explains the differences in the values presented in Figure 8.

4. Conclusions

There exists a very reasonable correspondence between the physical tensile test curves and their simulated counterparts in the plastic region up to the point of constriction. This correspondence was obtained despite the simulations having been performed on the assumption of homogeneous, defect-free materials and without the influence of microstructural parameters. Unlike the plastic region, the agreement between the actual curves and the simulations was not as good in the elas-

tic and elastic-plastic transition regions.

The rupture criterion adopted in the simulations was found to significantly affect the correspondence between the simulation and the experimental results. This stems from the different elongations which result from different rupture criteria. This suggests that the macroscopic elongation also has an important effect on the agreement between the results.

The values of the k and n parameters, obtained by linear regression using

a power function, were very similar to those determined in accordance with the ASTM E646-07 standard. This similarity shows that the easily applied linear regression method can be used to obtain these parameters.

Finally, the good correlation between the simulations and the physical tests in the plastic region suggests that the simulation method adopted in this work has significant potential for quick and precise application to the drawing process.

Acknowledgments

The authors would like to thank the Department of Metallurgical and Materi-

als Engineering of the UFOP School of Mines and the Gorceix Foundation for

financial support and the use of their laboratory facilities.

References

- AMERICAN SOCIETY FOR TESTING AND MATERIALS E646-07. Standard Test Methods for Tensile Strain-Hardening Exponents (n-Values) of Metallic Sheet Materials. USA: American Society for Testing and Materials, 2007.
- AMERICAN SOCIETY FOR TESTING AND MATERIALS E8M-04. Standard Test Methods for Tension Testing of Metallic Materials (Metric). USA: American Society for Testing and Materials, 1999.
- ARAÚJO, A.C. *Análise da formação de bandas de cisalhamento por meio de corpos-de-prova de tração especiais*. 2009. Belo Horizonte: Escola de Engenharia da Universidade Federal de Minas Gerais, 2009. 79p. (Dissertação de Mestrado em Engenharia Mecânica).
- CETLIN, P. R., HELMAN, H. *Fundamentos da conformação mecânica dos metais*. São Paulo: Artiliber, 2005. 170p.
- GARCIA, A., SPIM, J.A., SANTOS, C.A. *Ensaaios dos materiais*. (2ªed.) Rio de Janeiro: LTC- Livros Técnicos e Científicos Editora, 2012. 247p.
- HE, S., BAEL, A. V., LI, S. Y., HOUTTE, P. V., MEI, F., SARBAN, A. Residual Stress determination in cold drawn steel wire by FEM Simulation and X-Ray Diffraction. *Materials Science and Engineering A*, v. 346, p. 101-107, 2003.
- HUAN, Y.M., LU, S.C. Analysis of elliptical cup drawing process of stainless sheet metal. *Transactions of Nonferrous Metals Society of China*. China: St. John's University, Department of Mechanical and Computer-Aided Engineering, Jul. 2010. v. 21, n. 2, p. 371-377.
- KADKHODAYAN, M., MOAYYEDIAN, F. Analytical elastic-plastic study on flange wrinkling in deep drawing process. *Scientia Iranica Transactions B: Mechanical Engineering*. Sharif University of Technology, v.18, n. 2, p. 250-260. Jan. 2011.
- LAUDARES, F.A., CORRÊA, E.C.S., SANTOS, C.A., AGUILAR, M.T.P., CETLIN, P.R. Influência do coeficiente de atrito na determinação da tensão de refração através do método de elementos Finitos. In: CONGRESSO ANUAL DA ABM, 59, 2004. Belo Horizonte - MG. *Anais ...* São Paulo: Associação Brasileira de Metalurgia, Materiais e Mineração, 2004. p. 165-171.
- MARANGONI, A.L., MASSAROPPI JUNIOR, E. Correlação de ensaio de tração considerando os efeitos da taxa de deformação utilizando análises por elementos finitos. In: CBECIMAT - Congresso Brasileiro de Engenharia e Ciência dos Materiais, 22, 2016. Natal - RN. Retrieved in: <http://www.cbecimat.com.br/anais/PDF/404-055.pdf>. Accessed in: 20/11/2013
- MATH, M. Simulation and virtual reality – a key factor in future development of metal forming processes. Faculty of Mechanical Engineering and Naval Architecture – University of Zagreb, 2002. Retrieved in: <https://www.fsb.unizg.hr/deformiranje/math-keynotepaper.doc>. Accessed in: 18/11/2013.
- MENEZES, E. A. W. *Calibração de modelo numérico para simulação do comportamento mecânico de cabos poliméricos reforçados por fibra de carbono*. Porto Alegre: Escola de Engenharia, Universidade Federal do Rio Grande do Sul, 2015. 89 p. (Dissertação de Mestrado em Engenharia de Minas, Metalurgia e Materiais).
- SANTOS, C. E., MARTINS, N. Análise das propriedades mecânicas do aço TRIP 900 MC por meio do método de elementos finitos em comparação com ensaio de tração. In: IBERIAN LATIN AMERICAN CONGRESS ON COMPUTATIONAL METHODS IN ENGINEERING, 37, 2016. Brasília - DF. *Anais ...* Belo Horizonte: Brazilian Association of Computational Methods in Engineering, 2016. p. 6-9.
- SANTOS, C.A. *Simulação numérica da trefilação axissimétrica do aço inoxidável 420 considerando o efeito do caminho de deformação*. Belo Horizonte: Escola de Engenharia, Universidade Federal de Minas Gerais, 2005. 234 p. (Tese de Doutorado em Engenharia Metalúrgica e de Minas).

Received: 3 May 2015 - Accepted: 8 May 2016.